

Electron impact ionization of multicharged ions*

A. Salop

Molecular Physics Center, Stanford Research Institute, Menlo Park, California 94025

(Received 21 June 1976)

Computations have been made of the electron-impact ionization cross sections of multicharged ions of C, O, N, Ne, and Ar in the binary-encounter approximation. For ions of the four lighter species, the dominant ionization mechanism is that of direct electron ejection to the continuum. For Ar, excitation of inner-shell electrons to unoccupied bound levels with subsequent autoionization can also make a significant contribution to the total ionization process for some ions. The calculated binary-encounter values are in reasonable agreement with recent experimental data and with the quantum-mechanical calculations of Trefftz for O^{+4} and O^{+5} .

I. INTRODUCTION

The impact ionization of highly charged ions by electrons is an important process occurring in fusion plasmas¹ and in heavy-ion sources of various kinds.² Experimental investigations of such processes at the lower energies of interest have been hampered by the lack of suitable ion sources with most of the available data restricted to singly and doubly charged ions.³ Recently, however, innovative trapped-ion techniques have been developed and used in cross-section measurements on a few selected multicharged ions.⁴⁻⁷ Theoretical work on electron-ion impact ionization is also quite limited. It includes a few detailed quantum calculations,⁸⁻¹³ the use of a modified classical binary-encounter-approximation (BEA) model,¹⁴⁻¹⁶ and the development of a number of convenient semiempirical formulas.¹⁷⁻²⁰ These formulas are based primarily on modifications of the high-energy Bethe-Born formula²¹ for ionization with various parameters adjusted separately for each ion. They have been quite successful in representing the cross sections for singly charged ions of relatively low Z for which some experimental data are available.

In recent years, Donets and his group at Dubna have been successful in measuring total electron-impact ionization cross sections for highly charged ions of C, N, and Ar at an electron energy of about 2.5 keV using a cryogenically pumped electron-beam ionization source (EBIS) apparatus.⁴⁻⁶ These appear to be the first direct measurements of cross sections for highly stripped ions at such low energies. The Donets group finds that, for the lighter ions, single-electron ionization is clearly dominant, whereas for Ar^{+5} and Ar^{+6} , double-electron ionization also becomes important. It seems evident that for these heavier ions, the double-electron ionization primarily results from the production of inner L -shell vacancies by di-

rect electron continuum ionization followed by Auger transitions. Moreover, a significant contribution to the effective single-ionization cross section probably results from autoionization following the excitation of an inner L -shell electron to a state lying above the first continuum.

In response to the Dubna experiments, the trapped-ion measurements of Hasted and Awad,⁷ and the needs in a number of research areas for cross-section information on these processes, we have begun a program to obtain reasonable theoretical estimates of electron-impact ionization cross sections for a number of multicharged ions. The goal of our studies is to compute cross sections for various highly charged ions of several relevant atomic species with collision energies in the range from a few hundred to a few thousand eV appropriate to high-temperature fusion plasmas and to various types of heavy-ion sources. Clearly, the attainment of high accuracy in the calculation of these quantities would be an extremely difficult and time-consuming task, especially in view of the many cross sections desired. For many purposes, however, more approximate estimates with reliability of roughly a factor of two would be entirely adequate. In view of these considerations, we have made a series of computations using a modification of BEA theory adapted from the formulations of Thomas and Garcia¹⁴ and of Stabler.²² The model includes the effects of inner-shell ionization and excitation and Auger transitions. In this paper we present the results of such calculations for a number of multiply charged ions of C, N, O, Ne, and Ar.

II. METHOD OF CALCULATION

Although a classical approach is used in these studies, it is nevertheless convenient to consider a simplified central field model for the ions under study with electrons in each nl subshell regarded

as identical. Two dominant modes of ionization are considered: (1) direct transitions of outer- and inner-shell electrons to the continuum, and (2) excitation of inner-shell electrons to unoccupied bound levels lying above the first continuum, followed by autoionization. The first process can lead to the ejection of two or more electrons (multi-ionization) through Auger transitions if inner shells are involved. The second mechanism can similarly lead to multi-ionization if electrons in deep inner shells are excited. Thus, the total electron-impact ionization cross section Q^I , defined as the cross section for which the collision process results in the ejection of at least one electron, is given by

$$Q^I = Q^C + Q^A, \quad (1)$$

where Q^C , the contribution due to direct continuum ejection, is given by

$$Q^C = \sum_{n=n'}^N \sum_l \sigma_{nl}^C, \quad (2)$$

and Q^A , the cross section for the excitation-autoionization process is expressed as

$$Q^A = \sum_{n=n'}^{N-1} \sum_l \sigma_{nl}^A, \quad (3)$$

where σ_{nl}^C and σ_{nl}^A are the individual subshell cross sections corresponding to the two mechanisms. In these equations, N is the total number of shells and n' is the principal quantum number of the lowest shell for which the collision energy is greater than the corresponding threshold for ionization or excitation from that shell. For the excitation-autoionization process, $N \geq 2$. We can further write

$$\sigma_{nl}^A = A_{nl} \sigma_{nl}^E, \quad (4)$$

where σ_{nl}^E are the cross sections for excitation from each inner subshell and A_{nl} are the probabilities that an Auger transition will occur following the creation of the inner-shell vacancy.

For the ions and the corresponding collisional energy ranges considered in the present investigation, the ionization process is dominated by contributions from at most the two outermost shells. The excitation-autoionization process was found to be of importance only for ions of argon, where the inner shell is an L shell. In those cases, $A_{nl} \approx 1$ and σ_{nl}^A was taken equal to σ_{nl}^E . For convenient comparison with experiment, one can define for the argon ions studied here (up to Ar^{12+}), an effective single-electron and double-electron ionization cross section such that

$$Q_1 = \sigma_{3p}^C + \sigma_{3s}^C + \sigma_{2p}^A + \sigma_{2s}^A \quad (5)$$

and

$$Q_2 = \sigma_{2p}^C + \sigma_{2s}^C, \quad (6)$$

respectively. Thus, in those cases, single-electron ionization occurs as a combination of direct continuum ionization from the outer shell and autoionization following the excitation of an inner-shell electron. The double-electron process is assumed to result from a direct ionization of an inner-shell electron followed by an Auger transition, provided there are at least two electrons in the outer shell.

Note that in this treatment, we have neglected secondary processes contributing to ionization such as electron shakeoff²³ and direct two-electron ejection. On the basis of BEA estimates for atoms²⁴ and available experimental data,²⁵ the contribution from the latter process is probably at least two orders of magnitude smaller than that of direct single-electron ejection to the continuum. Shakeoff probabilities for these ions are expected, in general, to be smaller than 10%.

The individual subshell cross sections were computed using classical binary-encounter theory. For the direct continuum ionization cross sections σ_{nl}^C , we have used the BEA formulation for ions given by Thomas and Garcia.¹⁴ This is a modification of the classical BEA model originally formulated by Gryzinski^{24, 26, 27} for ionization of neutral atoms by charged-particle impact. In this modification, the effect of the residual ion field is taken into account both in increasing the kinetic energy of the projectile and in modifying its trajectory. We briefly outline the relevant theory and its extension to excitation using a notation appropriate to our application. All quantities are expressed in atomic units.

In this formulation, one can write the subshell ionization cross section (in units of πa_0^2) as

$$\sigma_{nl}^C = g_{nl} U_{nl}^{-2} S_C(\beta'_1, \beta_1) M_C(Z', \beta'_1, \beta_1). \quad (7)$$

Here U_{nl} is the binding energy of the nl subshell, g_{nl} is the number of subshell electrons, S_C is a reduced cross section, and M_C is an explicit magnification factor associated with the curvature of the incident electron in the residual field of the ion with effective charge Z' . The reduced energy parameters β_1 and β'_1 are given by the ratios E_1/U_{nl} and E'_1/U_{nl} , where E_1 is the initial kinetic energy of the incident electron and E'_1 is its kinetic energy at the binary encounter after acceleration in the residual field of the ion. This latter quantity is determined by assuming that if the binary collision resulting in ionization (energy transfer $\Delta E > U_{nl}$) occurs at the distance ξ from the target nucleus, the resultant projectile electron

kinetic energy becomes

$$E'_1 = E_1 + Z'/\xi \geq E_1. \quad (8)$$

Both the collision radius ξ and the magnification factor M_C are obtained by Thomas and Garcia¹⁴ using a classical model for energy exchange between a pair of colliding electrons. The reduced cross section S_C appearing in Eq. (7) has been averaged over the speed distribution of the target electrons. In the present studies, a δ -function speed distribution was assumed for the subshell electrons with $v = (2U_{nl})^{1/2}$. The resulting cross sections are close to those obtained with a hydrogenic speed distribution.^{15, 16}

Thomas and Garcia find that their cross sections for singly charged ions are in better accord with experiment at lower collision energies, if, in the computation of S_C , the quantity β'_1 is given by the relation

$$\beta'_1 = \beta_1 + 2 \quad (9)$$

rather than by the direct determination following from Eq. (8). The latter modification results in values that are lower in the region of the cross-section maxima, but that correspond closely to the directly obtained cross sections at higher energies. The procedure appears to simulate exchange effects in some way, and we have used it consistently in the calculation of S_C . However, directly determined values for β'_1 were still used in the computation of the magnification factors.

With the introduction of this modification for β'_1 and the use of the δ -function speed distribution, the following remarkably simple relation for S_C is obtained and is applicable throughout the range of validity of the BEA model

$$S_C(\beta'_1, \beta_1) = (1/\beta'_1) \left[\frac{2}{3}(1 - \beta_1^{-2}) + 1 - 1/\beta_1 \right]. \quad (10)$$

The excitation cross sections σ_{nl}^A for the inner-shell target electrons were also calculated in the BEA, based primarily on the formulation of Stabler²² with similar modifications for the effects of the residual ion field. In the context of our application, rather than excitation to a particular bound level, we are concerned with the cross section for excitation of inner-shell electrons to all unoccupied bound levels corresponding to energy transfers ΔE to the target electron such that

$$E_{nl}^b \leq \Delta E \leq U_{nl}, \quad (11)$$

where E_{nl}^b is the energy of the lowest available bound level relative to the energy of the inner nl level of the target electron. The expression for σ_{nl}^A is given by an equation similar to Eq. (7), but with S_C replaced by a reduced excitation-autoionization cross section S_A , and M_C replaced by

a magnification factor M_A appropriate to the excitation process. The expression for M_A is derived analogously to that for M_C , but with the assumption of an electron-electron collisional energy transfer corresponding to the minimum excitation energy E_{nl}^b . The resulting equation is identical to that obtained in the case of ionization except that the electron-electron separation parameter designed as Δ in Eq. (13) of Ref. 14 is now given by

$$\Delta = (\beta_1 - \alpha_{nl})^{-1} [(\beta_1/\alpha_{nl} - 1)^{1/2} + 1], \quad (12)$$

where $\alpha_{nl} = E_{nl}^b/U_{nl}$.

Here also, with the assumption of a δ -function speed distribution and the empirical modification for β'_1 [Eq. (9)], a very simple expression for S_A is obtained, with the threshold given by $\beta_1 = \alpha_{nl}$:

$$S_A(\beta'_1) = (2/3\beta'_1)(1/\alpha_{nl} - 1)(1/\alpha_{nl} + 2.5). \quad (13)$$

Previous work indicates that the computation of excitation cross sections by classical BEA theory leads to results that are distinctly less satisfactory than the corresponding calculations for ionization.²² Nevertheless, the approach does appear to give cross sections in fair agreement with experimental information over a restricted range of collision energies, if we may be guided by the case of the electron-hydrogen collisions. Table I compares values of BEA total electron-impact excitation cross sections for H(1s) with values that were derived from experimental measurements of the cross sections for H(1s-2p) excitation²⁸ (which dominates the excitation process). The total excitation cross sections were estimated by multiplying each experimental 1s-2p value by a factor equal to the ratio of total excitation cross section to the 1s-2p excitation cross section obtained from the extended Bethe-Born theory given by Omidvar and Khateeb.²⁹ The two

TABLE I. e -H excitation cross sections.

Electron energy (eV)	Experimental ^a (10^{-17} cm ²)	BEA (10^{-17} cm ²)
40	8.3	10.2
50	8.2	8.2
60	7.8	6.8
80	7.4	5.1
100	7.1	4.1
120	6.5	3.4
140	5.9	2.9
160	5.8	2.6
180	5.6	2.3
200	5.3	2.0

^a Experimental values from Ref. 28 multiplied by ratio of total to 1s-2p excitation cross sections derived from theory of Ref. 29.

sets of values agree to within a factor of 2 over a range of collision energies up to about 12 times threshold. The BEA cross sections decrease more rapidly at higher energies, however, with a fall-off characteristic of a $1/E_1$ energy dependence whereas the experimental values are expected to decrease as $\log(E_1/E_1)$ at sufficiently high energies.

In view of these considerations, and because for most of the ions studied in this work the contribution due to autoionization is usually much smaller than the direct continuum ionization, it seemed reasonable to use the convenient BEA approach to estimate excitation cross sections also. The range of collision energies in all cases where excitation-autoionization contributed significantly to ionization was restricted to collision energies below ten times threshold.

III. COMPUTATIONS AND DISCUSSION

A. Computational procedure

Ionization cross sections for C, N, O, Ne, and Ar ions were computed using the modified BEA theory previously outlined. For the four lighter species, the Roothaan-Hartree-Fock orbital energies of Clementi and Roetti³⁰ were taken as the binding energies for the various subshells. For Ar ions, where some excited-state binding energies were required, the binding energies used were the nl orbital energies obtained by numerically solving the radial Schrödinger equation with the independent-particle-model potential for ions as given by Green *et al.*³¹ We have made the assumption throughout that dipole-allowed transitions dominate the excitation and have chosen the parameters E_{ni}^b , the lowest accessible bound level [Eq. (11)], in accordance with this assumption. For the lighter ions, for which continuum ionization dominates, the cross sections were computed over a range of collision energies that was usually restricted to values smaller than 40 times threshold. For Ar, where autoionization appeared to be an important contribution for some ions, the maximum collision energy was always smaller than 10 times the inner-shell excitation threshold.

B. Comparison with the measurements by the Donets group

Comparisons between experimentally obtained total ionization cross sections of Donets⁴ and our BEA values are given in Table II for C ions at 2500 eV and N ions at 2100 eV, respectively. For the C^{+2} ion, this collision energy is rather high in terms of the applicability of BEA theory, and the

TABLE II. Comparison of experimental^a and BEA total electron-impact ionization cross sections for C and N ions.

Ion	Collision energy (keV)	Q^I (10^{-20} cm ²)	
		Experimental ^a	BEA
C^{+2}	2.5	200	202
C^{+3}	2.5	57	83
C^{+4}	2.5	30	17
C^{+5}	2.5	14	6.4
N^{+3}	2.1	125	143
N^{+4}	2.1	39	62
N^{+5}	2.1	9	12
N^{+6}	2.1	4	4.6

^aReference 4.

estimated cross section is probably somewhat low. In all cases for these ions, and also for O and Ne ions, where the only inner shell is a K shell, contributions to overall ionization due to the excitation-autoionization mechanism are small compared with direct continuum ionization and are not included in the total cross-section determinations.

The C^{+2} and N^{+3} BEA cross sections include a contribution due to double-electron ionization (K -shell ionization with subsequent Auger transition). However, in both cases, the K -shell contributions are not more than 10% of the total ionization cross sections. The agreement between the BEA and experimental values (which were derived from the experimental data assuming only single-electron ionization) is well within a factor of 2 for all values except for that of C^{+5} .

An apparent inconsistency is noted in the observed experimental values for the hydrogenic ions C^{+5} and N^{+6} and the helium-like ions C^{+4} and N^{+5} . If we label quantities referring to C ions with a subscript CA and those referring to N ions with a subscript N, then the ratio R of the cross sections for C^{+5} and N^{+6} can be written roughly (on the basis of the high-energy theory) as

$$R = Q_{CA}/Q_N \approx (E_N Z_N^2 M_{CA}) / (E_{CA} Z_{CA}^2 M_N), \quad (14)$$

where E is the electron kinetic energy, Z is the nuclear charge, and M the focusing or magnification factor,^{14, 20} which for C^{+5} is about 1.16 and for N^{+6} about 1.13. On this basis, one would expect the C^{+5} cross section to be larger than the N^{+6} cross section by roughly 1.2. For the BEA values, the ratio is 1.39, whereas for the experimental value it is 3.5, which seems to be clearly out of line. Similar considerations apply to the cross sections for the helium-like ions.

Finally, the presence of metastable ions formed by electron-impact processes can be a disturbing complication in these measurements. Unfortu-

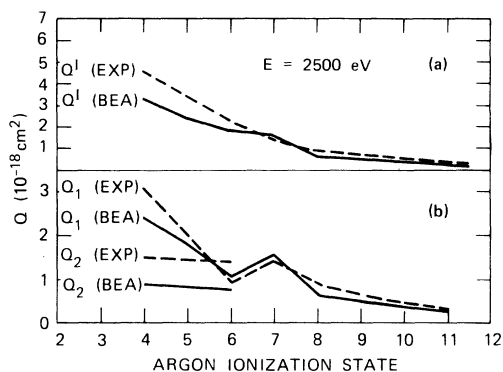


FIG. 1. Comparison between experimental and BEA ionization cross sections for electrons colliding with Ar in several charge states at an energy of 2500 eV. The upper curves (a) are the total cross sections equal to the sum of the individual cross sections for single and double ionization $Q^I = Q_1 + Q_2$. The lower curves (b) are the individual single- and double-ionization cross sections Q_1 and Q_2 , respectively. The dashed curves show the experimental data obtained from Ref. 4, and the solid lines represent the calculated BEA cross sections.

nately, these effects are difficult to evaluate or correct for.

Comparisons between experimental and theoretical BEA electron-impact ionization cross sections for several Ar ions at a collision energy of 2500 eV are presented in Fig. 1. For these ions both *M*- and *L*-shell interactions are involved (the collision energy is too low for *K*-shell ionization), and one must take into account the effects of Auger transitions following inner-shell ionization and excitation. Figure 1(a) is a comparison between the experimental and BEA total cross sections for a range of charge states, whereas Fig. 1(b) is a breakdown into the single- and double-ionization components, Q_1 and Q_2 , respectively. According to our model, double ionization can occur only for charge states 4, 5, and 6 for which there are at least two electrons in the outer shell. This appears to be substantiated by the experimental results. The agreement between $Q_1(\text{exp})$ and $Q_1(\text{BEA})$ is quite good (within 31%) over the entire range of charge states in-

TABLE III. Estimated ionization cross sections σ^C and σ^A for various ions of Ar at 2.5 keV collision energy.

Ion	σ^C (10^{-18} cm 2)	σ^A (10^{-18} cm 2)
Ar $^{+4}$	3.06	0.25
Ar $^{+5}$	2.09	0.30
Ar $^{+6}$	1.41	0.35
Ar $^{+7}$	0.96	0.60

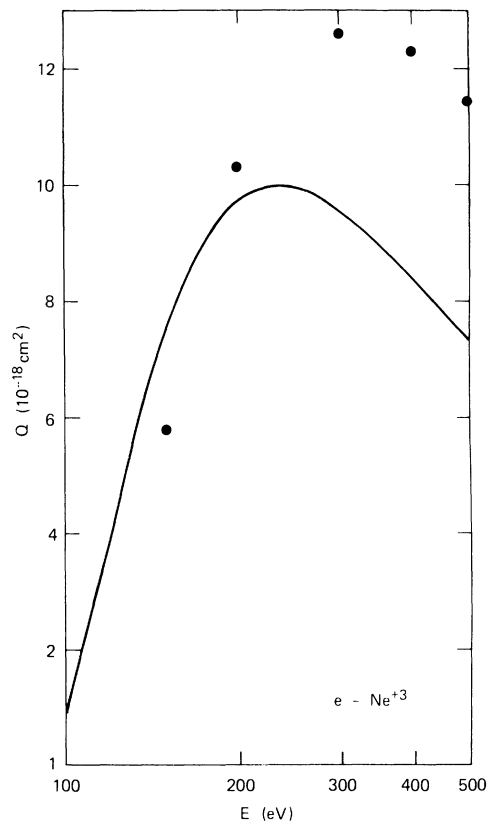


FIG. 2. Ionization cross sections for electrons colliding with Ne^{+3} in the collisional energy range between 100 and 500 eV. The circles represent experimental data taken from Ref. 7. The solid curves are the BEA results obtained in this work.

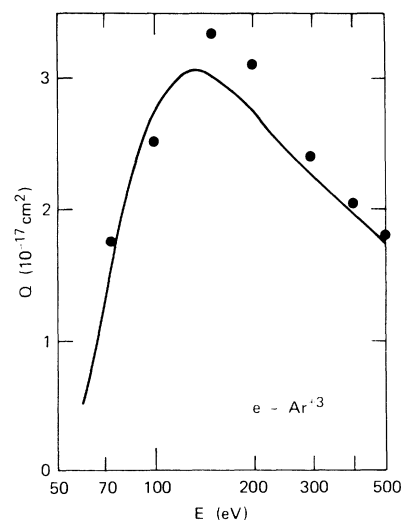


FIG. 3. Ionization cross sections for electrons colliding with Ar^{+3} in the collisional energy range between 60 and 500 eV. The circles represent the experimental data taken from Ref. 7. The solid curves are the BEA results obtained in this work.

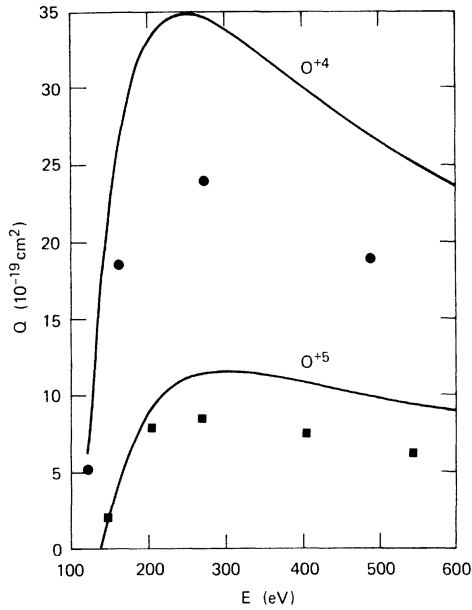


FIG. 4. Ionization cross sections for electrons colliding with O^{+4} and O^{+5} in the collisional energy range between 100 and 600 eV. The circles are the cross sections for O^{+4} given by Trefftz in Ref. 9 calculated using a distorted-wave approximation. The squares are values for O^{+5} also given in Ref. 9 obtained using a Coulomb-Born-Oppenheimer method. The solid curves are the BEA results computed in the present study.

cluding the rise in single ionization noted for charge state 7. The latter feature can be explained as follows. For charge states 4, 5, and 6, the overall single-electron ionization is a combination of M -shell continuum ionization and autoionization following L -shell excitation. For charge state 7, these contributions are also present, but there is also a substantial additional contribution due to direct

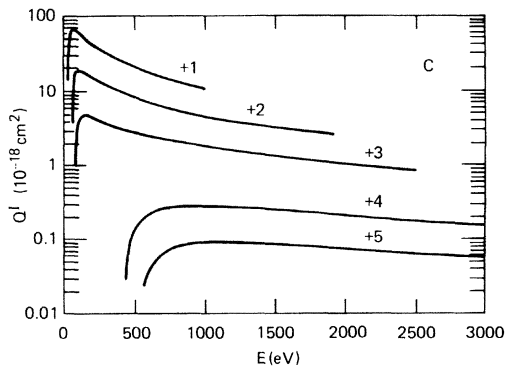


FIG. 5. BEA electron-impact ionization cross sections for C ions. Each curve is labeled by the charge state of the target ion.

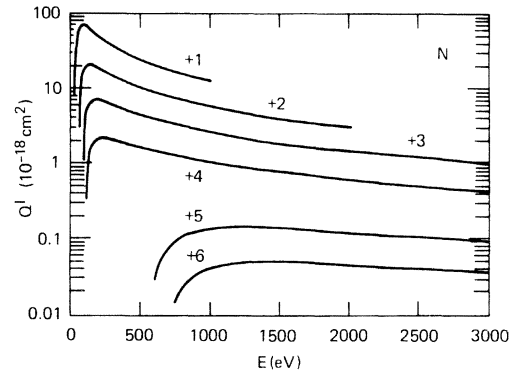


FIG. 6. BEA electron-impact ionization cross sections for N ions. Each curve is labeled by the charge state of the target ion.

continuum ionization from the L shell giving rise to a jump in Q_1 . The latter process also exists for charge states 4, 5, and 6, but in these cases it ultimately results in two-electron emission because of Auger transitions. The subsequent drop-off of the cross section at charge state 8 occurs because of the complete elimination of the M -shell contribution.

The correspondence between $Q_2(\text{BEA})$ and $Q_2(\text{exp})$ is much less satisfactory although agreement is still within a factor of 2 and the charge-state dependence is similar for the two sets of values.

Table III lists the calculated values of σ^C and σ^A for the ions of argon with charge states 4 to 7. According to these estimates, direct continuum ionization dominates over the excitation-autoionization process except for Ar^{+7} where the two contributions are roughly comparable.

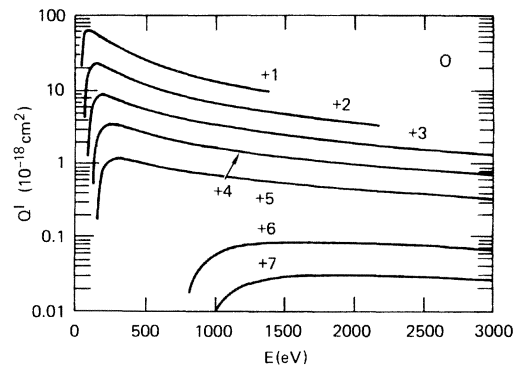


FIG. 7. BEA electron-impact ionization cross sections for O ions. Each curve is labeled by the charge state of the target ion.

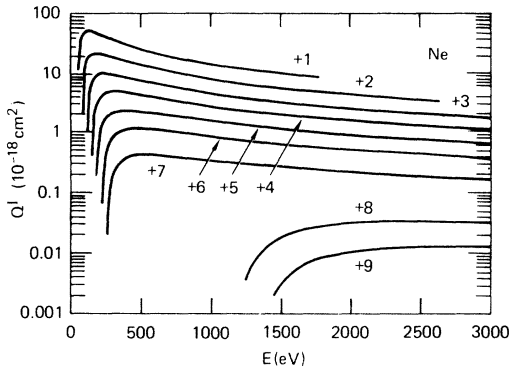


FIG. 8. BEA electron-impact ionization cross sections for Ne ions. Each curve is labeled by the charge state of the target ion.

C. Comparison with the measurements by the Hasted group

The previous work on singly-ionized ions^{14, 15} has indicated that the BEA cross sections are relatively poor in the region of the threshold and the cross-section maximum. In general, the computed cross sections considerably overestimate the experimental values at these energies. In Figs. 2 and 3, we compare BEA cross sections for Ne^{+3} and Ar^{+3} in the low-energy region with the measured values of Hasted and Awad.¹⁴ The agreement is quite adequate for these multicharged ions, well within a factor of 2, although the computed cross sections peak at lower energies than the experimental values and show lower maximum values.

D. Comparison with the calculations by Trefftz

Similarly, in Fig. 4 comparison is made between low-energy BEA computations for O^{+4} and O^{+5} and earlier calculations by Trefftz⁹ using a distorted-wave method for O^{+4} and a Coulomb-Born technique for O^{+5} . The latter calculations include exchange. Here also, quite adequate agreement is observed, although the BEA results are distinctly higher.

E. Extended BEA cross-section computations

In view of the reasonable agreement noted between the available experimental and theoretical data for multicharged ions and the BEA calculations, it seemed useful to make the computations for ions of several atomic species over an ex-

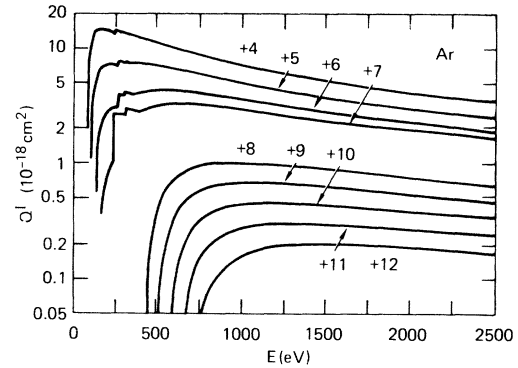


FIG. 9. BEA electron-impact ionization cross sections for several Ar ions. Each curve is labeled by the charge state of the target ion.

tended energy range. In Figs. 5 to 8, curves of total electron-impact ionization cross sections for various ions of C, N, O, and Ne are presented for a range of energies appropriate to the BEA theory. Similar curves in a more restricted energy range are also given for various multicharged Ar ions in Fig. 9.

For each atomic species, the cross sections decrease in magnitude with increase in charge state. A shell effect is apparent, with the largest decrease occurring after the last outer-shell electron is stripped off. For Ar, three breaks can be seen at low energies in the upper set of curves. These are particularly noticeable for Ar^{+6} and Ar^{+7} . The first and second breaks are due to the onset of the excitation-autoionization process for the inner $2p$ and $2s$ subshells. The third, more gradual feature is due to the onset of direct L -shell impact ionization.

IV. CONCLUDING REMARKS

We have used modified BEA theory to compute electron-impact ionization cross sections for a number of highly charged ions. For several charge states of Ar, Auger transitions following inner-shell excitation and ionization events were found to contribute significantly to the overall ionization. Our results compare favorably with the available experimental data, with agreement significantly better than a factor of 2 in most cases. The method thus appears to be a useful and convenient one for rapid evaluation of many of the electron-impact cross sections in the analysis of high-temperature plasma systems.

*Work supported in part by the U. S. Energy Research and Development Administration under Contract AT(04-3)-115 and in part by Stanford Research Independent Research and Development Funds.

¹E. Hinnov, *Bull. Am. Phys. Soc.* 21, 509 (1976).

²A. Septier, *IEEE Trans. Nucl. Sci.* NS-19, 22 (1972).

³See G. H. Dunn, in *IEEE Trans. Nucl. Sci.* NS-23, 929 (1976), for a comprehensive list of publications reporting experimental work in this area.

⁴E. D. Donets, *IEEE Trans.* NS-23, 897 (1976).

⁵E. D. Donets and V. I. Ilyushchenko, Joint Institute of Nuclear Research (Dubna) Report No. P7-8310, 1974 (unpublished).

⁶E. D. Donets, A. I. Pikin, Joint Institute of Nuclear Research (Dubna) Report No. P7-9243, 1975 (unpublished).

⁷J. B. Hasted and G. L. Awad, *J. Phys. B* 5, 1719 (1972).

⁸F. B. Malik and E. Trefftz, *Naturforsch.* 16a, 583 (1961).

⁹E. Trefftz, *Proc. R. Soc. Lond. A* 271, 379 (1963).

¹⁰A. Burgess and M. R. H. Rudge, *Proc. R. Soc. Lond. A* 273, 372 (1963).

¹¹P. G. Burke and A. J. Taylor, *Proc. R. Soc. Lond. A* 287, 105 (1965).

¹²M. R. H. Rudge and S. B. Schwartz, *Proc. Phys. Soc. Lond.* 88, 563 (1966).

¹³O. Bely and S. B. Schwartz, *Astron. Astrophys.* 1, 281 (1969).

¹⁴B. K. Thomas and J. D. Garcia, *Phys. Rev.* 179, 94 (1969).

¹⁵K. C. Mathur, A. N. Tripathi, and S. K. Joshi, *Phys.*

Rev. 184, 242 (1969).

¹⁶K. C. Mathur, A. N. Tripathi, and S. K. Joshi, *Astrophys. J.* 165, 425 (1971).

¹⁷W. Lotz, *Z. Phys.* 206, 205 (1967); 216, 241 (1968).

¹⁸H. W. Drawin, *Z. Phys.* 164, 513 (1961).

¹⁹O. Bely and P. Faucher, *Astron. Astrophys.* 18, 487 (1972).

²⁰See D. N. Tripathi and D. K. Rai, *J. Quant. Spectrosc. Radiat. Transfer* 11, 1665 (1971), for a listing and critical discussion of various empirical methods.

²¹M. Inokuti, *Rev. Mod. Phys.* 43, 297 (1971).

²²R. C. Stabler, *Phys. Rev.* 133, A1268 (1964).

²³T. A. Carlson, C. W. Nestor, Jr., T. C. Tucker, and F. B. Malik, *Phys. Rev.* 169, 27 (1968).

²⁴M. Gryzinski, *Phys. Rev.* 138, A336 (1965).

²⁵H. E. Stanton and J. E. Monahan, *Phys. Rev.* 119, 711 (1960).

²⁶M. Gryzinski, *Phys. Rev.* 115, 374 (1959); 138, A305 (1965); 138, A332 (1965).

²⁷L. Vriens, in *Case Studies in Atomic Collision Physics I*, edited by E. W. McDaniel and M. R. C. McDowell (North-Holland, Amsterdam, 1969), p. 337.

²⁸W. L. Fite and R. T. Brackmann, *Phys. Rev.* 112, 1151 (1958).

²⁹K. Omidvar and A. H. Kateeb, *J. Phys. B* 6, 341 (1973).

³⁰E. Clementi and C. Roetti, *At. Data Nucl. Data Tables* 14, 177 (1974).

³¹A. E. S. Green, R. H. Garvey, and C. J. Jackson, *Int. J. Quantum Chem. Symp.* 9, 43 (1975).